Phase Behavior and Nanoscale Structure of Phospholipid Membranes Incorporated with Acylated C_{14}-Peptides

Tina B. Pedersen,*† Thomas Kaasgaard,†‡§ Morten Ø. Jensen,‡ Sven Frokjaer,* Ole G. Mouritsen,‡ and Kent Jørgensen†

*Department of Pharmaceutics, The Danish University of Pharmaceutical Sciences, DK-2100 Copenhagen Ø, Denmark; †Department of Chemistry, Technical University of Denmark, DK-2800 Lyngby, Denmark; ‡MEMPHYS—Center for Biomembrane Physics, University of Southern Denmark—Odense, DK-5230 Odense M, Denmark; and §CSIRO Molecular & Health Technologies, North Ryde, NSW 2113, Australia

ABSTRACT The thermotropic phase behavior and lateral structure of dipalmitoylphosphatidylcholine (DPPC) lipid bilayers containing an acylated peptide has been characterized by differential scanning calorimetry (DSC) on vesicles and atomic force microscopy (AFM) on mica-supported bilayers. The acylated peptide, which is a synthetic decapeptide N-terminally linked to a C_{14} acyl chain (C_{14}-peptide), is incorporated into DPPC bilayers in amounts ranging from 0–20 mol %. The calorimetric scans of the two-component system demonstrate a distinct influence of the C_{14}-peptide on the lipid bilayer thermodynamics. This is manifested as a concentration-dependent downshift of both the main phase transition and the pretransition. In addition, the main phase transition peak is significantly broadened, indicating phase coexistence. In the AFM imaging scans we found that the C_{14}-peptide, when added to supported gel phase DPPC bilayers, inserts preferentially into preexisting defect regions and has a noticeable influence on the organization of the surrounding lipids. The presence of the C_{14}-peptide gives rise to a laterally heterogeneous bilayer structure with coexisting lipid domains characterized by a 10 Å height difference. The AFM images also show that the appearance of the ripple phase of the DPPC lipid bilayers is unaffected by the C_{14}-peptide. The experimental results are supported by molecular dynamics simulations, which show that the C_{14}-peptide has a disordering effect on the lipid acyl chains and causes a lateral expansion of the lipid bilayer. These effects are most pronounced for gel-like bilayer structures and support the observed downshift in the phase-transition temperature. Moreover, the molecular dynamics data indicate a tendency of a tryptophan residue in the peptide sequence to position itself in the bilayer headgroup region.

INTRODUCTION

The interaction and association of peptides and proteins with lipid membranes can be significantly modulated by using covalently attached hydrocarbon chains as hydrophobic anchors. The use of hydrophobic anchors provided by, e.g., acylation or prenylation, is a common strategy used by biological membranes to attach peptides and proteins to the lipid bilayer to localize them into regions, such as lipid domains and rafts, for which the anchoring moiety has a special affinity (1–3). Acylation is a particularly interesting anchoring mechanism since it can be enzymatically modified and hence be used for regulation by relocating the proteins at the membrane surface or within a laterally differentiated membrane structure, e.g., in relation to rafts. Many peripheral membrane proteins involved in cell signaling, e.g., protein kinases C substrate (MARCKS) and Src proteins, are attached to the membrane by a combination of a hydrocarbon chain that interacts with the hydrophobic core of the membrane and positively charged amino acids that interact electrostatically with negatively charged lipid headgroups or have aromatic residues that localize at the membrane-water interface (4–6). Other peripheral proteins, such as Src family kinases, HIV-1, Gag Nef, and cytochrome *c*, use similar strategies, furthermore in a way that may be controlled by the lateral structure of the cellular membrane (1,7). Finally, the efficacy of some peptide drugs and hormones can be substantially enhanced by acylation (8,9).

Research in the physical properties of lipid membranes has shown that lipid membranes are highly structured fluids that are characterized by small-scale structures, which are of importance for membrane function (10–13). A quantitative characterization of lateral membrane structure, e.g., by the use of detailed imaging or computer simulation calculations, is therefore of interest, in particular in the presence of peptides and proteins. It has been shown that the function of several membrane-associated enzymes and proteins is strongly influenced by the physical properties and phase behavior of the lipid membrane (14–17). One striking example is the activity of the water-soluble phospholipase A_2 (PLA_2) enzyme. Both experimental and simulation results have demonstrated that the activity of PLA_2 depends strongly on the physical state and microstructure of the lipid-membrane substrate (18,19). In particular, it has been shown that the activity is strongly enhanced in the vicinity of the main phase transition, where the lipid membrane shows a high degree of heterogeneity with coexisting domains of gel and fluid phase lipid structures. The potency of other compounds such as general anesthetics and various insecticides has also been related to their capacity for altering lipid membrane structure and dynamics (20,21). In a pharmaceutical context it is therefore of interest to study the perturbing effect that acylated

Submitted February 5, 2005, and accepted for publication July 5, 2005.

Address reprint requests to Kent Jørgensen, E-mail: jorgense@kemi.dtu.dk.

0006-3495/05/10/2494/10 $2.00

doi: 10.1529/biophysj.105.060756

peptides may have on the macroscopic as well as the microscopic phase structure of lipid membranes.

Saturated phospholipid membranes undergo several thermally induced phase transitions. The most studied transition is the main phase transition, which takes the membrane from a low-temperature gel phase, characterized by a high degree of acyl-chain order, to a high-temperature fluid phase in which the acyl chains have a substantial degree of conformational disorder. Below the main phase transition, saturated phosphatidylcholine membranes undergo a low-enthalpy transition called the pretransition. The pretransition is most pronounced in DSC scans of multilamellar liposomes, but has also been reported in unilamellar liposomes. Several studies have demonstrated that the occurrence of the pretransition is sensitive to the addition of various molecular compounds, such as cholesterol, gramicidin S, ursodeoxycholic, and alphaxalone (22–25). Between the pre- and the main phase transitions, the lipid bilayers are characterized by regular corrugations with a periodic spatial distribution referred to as the ripple phase (26–28).

In this study, we investigate general implications on phase behavior and bilayer structure due to the interactions between an acylated synthetic model peptide with DPPC bilayers. Given that several important biological functions rely on acylated peptides as already stated above, in-depth insight into the resulting phase behavior and nanoscale structure of the membrane within such complexes is therefore of fundamental interest. This cationic deca-peptide is N-terminally linked to a myristoyl fatty acid and will be denoted C_{14}-peptide in the following, where C_{14} refers to the 14-carbon acyl chain of myristoyl fatty acid. The choice of model peptide was motivated for reasons of simplicity. The short peptide could easily be synthesized and myristylated. It was chosen to have a proline residue in the middle to arrange for the simplest element of secondary (hairpin) structure, which in principle provides a means of experimental monitoring of conformational changes, e.g., hairpin-coil transitions likely occurring at the lipid-water interface (29). A tryptophan residue was positioned adjacent to the membrane anchor, i.e., at the interface, to provide a feasible route for spectroscopic localization of the anchor, but it was not introduced for explicit anchoring purposes. In our previous study (29), we showed by means of IR spectroscopy that the cationic C_{14}-peptide assumes in solution a hairpin structure and by means of calorimetric studies that it interacts stronger with lipid membranes containing anionic lipids as compared to pure zwitterionic DPPC membranes. However, the appearance of a second small peak around 30°C in the heat capacity curves of C_{14}-peptide/DPPC unilamellar liposomes indicated that the C_{14}-peptide had a distinct influence on the phase structure of the DPPC bilayers. As a result, further studies were undertaken to elucidate the interaction of the C_{14}-peptide with DPPC lipid membranes. The aim of this study is to gain further insight into both the macroscopic and microscopic lipid bilayer structure of the binary systems composed of DPPC and C_{14}-peptide with particular focus on the second small peak arising around 30°C. We have used differential scanning calorimetry (DSC) to study the thermodynamic phase behavior of DPPC liposomes containing variable amounts of the C_{14}-peptide and show that the second small peak is in fact the pretransition, which is shifted to lower temperatures by the C_{14}-peptide. This indicates that the C_{14}-peptide stabilizes the ripple phase. In other previous studies it was shown that the ripple phase can be visualized by atomic force microscopy (AFM) by using a sample preparation technique that produces solid supported double bilayers (30–32). Thus, to obtain a microscopic understanding of the macroscopic phase behavior, we have used this technique to investigate by AFM the nanoscale lateral organization of the mixed bilayers composed of C_{14}-peptide and DPPC. The experimental findings are supported by molecular dynamics (MD) simulations carried out to investigate the interaction of the C_{14}-peptide with DPPC lipid membranes as previously reported in detail confirming, e.g., a transient hairpin structure of the C_{14}-peptide at the lipid interface (33).

MATERIALS AND METHODS

Materials

1,2-dipalmitoyl-*sn*-glycero-3-phosphocholine (DPPC) was obtained from Avanti Polar Lipids (Alabaster, AL). Myristoyl-HWAHPGGHHA-amide (C_{14}-peptide) >98% purity was purchased from Commonwealth Biotechnologies, (Richmond, VA). All other chemicals were of reagent grade and used without further purification.

Liposome preparation

Multilamellar vesicles (MLVs) were made by dissolving and mixing DPPC and C_{14}-peptide in a chlorofom/methanol mixture (1:1). The solvent was evaporated using a gentle stream of nitrogen, followed by drying at low pressure overnight. For the DSC experiments the thin lipid film was hydrated in a buffer solution containing 10 mM 2-morpholinoethanesulfonic acid (MES), 50 mM KCl, and 1 mM NaN_3, (pH = 5.8). For the AFM studies, the thin lipid film was hydrated with milli-Q-water. Large unilamellar vesicles (LUVs) were made by extrusion of the MLV suspension 10 times through two stacked 100 nm Nuclepore polycarbonate filters (Whatman, Brentford, UK) (34). In addition to experiments where the C_{14}-peptides were incorporated from the organic phase, experiments were also conducted where the C_{14}-peptides dissolved in MES-buffer were added to the water phase of preformed liposomes.

Differential scanning calorimetry

Heat capacity curves were obtained using an N-DSC II differential scanning calorimeter (Calorimetry Sciences, Provo, UT). Liposome suspensions were made of 3 mM lipids including appropriate amounts of the C_{14}-peptide incorporated from the organic phase or added to the water phase of preformed liposomes. The samples were equilibrated for 1 h at the starting temperature and heat capacity curves were obtained at a scanning rate of 30°C/h.

Preparation of supported bilayers

Supported lipid bilayer membranes containing DPPC and C_{14}-peptide were obtained by bath sonication using a Bransonic ultrasonic cleaner (Branson

Ultrasonics, Danbury, CT) of the MLV suspension for 50 min at 50°C, yielding small unilamellar vesicles (SUV). The SUV suspension was transferred to a home-built cell for the atomic force microscope containing freshly cleaved mica and then incubated for 1 h at 37°C. The sample was subsequently rinsed 10 times with a 20 mM NaCl solution. In this way supported bilayers were obtained, which were often partly covered by a second bilayer. Pure DPPC bilayers were obtained by probe sonication of the MLV suspension using a Labsonic U tip sonicator (B. Braun Biotech International, Melsungen, Germany), followed by centrifugation at 5500 rpm for 8 min to remove titanium residuals. The supernatant was immediately reheated to 60°C, and the obtained SUV suspension was transferred to the home-built cell containing freshly cleaved mica. The SUV suspension was incubated for 1 h at 37°C and was washed 10 times with a 20 mM NaCl solution.

AFM

AFM studies were performed using a PicoSPM atomic force microscope (Molecular Imaging, Phoenix, AZ). Contact mode topographic and deflection mode images were recorded using oxide sharpened silicon nitride cantilevers (ThermoMicroscopes, Sunnyvale, CA) with nominal spring constants of 0.01 N/m. In the experiments where the C_{14}-peptide was added to preformed lipid bilayers (see Figs. 3 and 5), 15 μL of a 0.1 mg/mL C_{14}-peptide solution was added to the home-built fluid cell for the AFM, having a volume of ~0.6 mL.

MD simulations

The MD simulations were carried out using the program NAMD (35) with the CHARMM27 parameter set (36–38). The simulations involved 71 phospholipid molecules and 2092 water molecules for each C_{14}-peptide corresponding to a peptide concentration of 1.4 mol %. All MD simulations were carried out for 14 ns at 52°C under a range (35–70 dyn/cm) of applied tensions imposed to mimic gel-like as well as fluid-like states of the model. This approach, derived from Feller et al. (39), is justified and described in detail elsewhere (33).

RESULTS AND DISCUSSION

Phase behavior of DPPC liposomes premixed with C_{14}-peptide

Fig. 1 *A* shows DSC heating curves of DPPC multilamellar liposomes incorporated with increasing amounts of the C_{14}-peptide. The heat capacity curve of the pure DPPC liposomes displays a main phase transition at 41.9°C. The main phase transition temperature, T_m, and the half-height width of the transition, $T_{1/2}$, are affected by increasing concentrations of the C_{14}-peptide as seen from the values listed in Table 1. At concentrations of 10 and 15 mol % C_{14}-peptide, a low-temperature shoulder appears on the main phase transition peak, and at 20 mol % C_{14}-peptide two melting peaks can be observed, indicating phase separation. The melting enthalpy, ΔH, which is determined as the area under the C_p-curves in Fig. 1 *A*, is listed in Table 1. It is noted that the transition enthalpy decreases significantly when the concentration of the C_{14}-peptide in the liposomes increases.

Fig. 1 *B* shows the same DSC scans as Fig. 1 *A*, with focus on the temperature range where the pretransition takes place. Multilamellar DPPC liposomes (0 mol % peptide) display a pretransition peak at 36.1°C. As the concentration of the C_{14}-peptide increases, the pretransition temperature is shifted to lower temperatures and the transition is broadened. At 15 mol % C_{14}-peptide the pretransition temperature is downshifted almost 10°C compared to the pretransition of pure DPPC multilamellar liposomes and now appears at 27.2°C. At 20 mol % the pretransition is completely abolished. It is seen that the pretransition temperature is downshifted much more dramatically than the main phase transition. Thus, the temperature range where the ripple phase appears is expanded by the presence of the C_{14}-peptide. Interestingly, Wang et al. (40) have shown by x-ray diffraction and freeze-fracture electron microscopy that a ripple phase is present in mixtures of phospholipids and lipidated α-tocopherol well below the pretransition temperature of the corresponding pure phospholipid.

Phase behavior of DPPC liposomes after incorporation of the C_{14}-peptide from the aqueous phase

In the previous paragraph we described the effect of the C_{14}-peptide when it was premixed with the DPPC lipids during

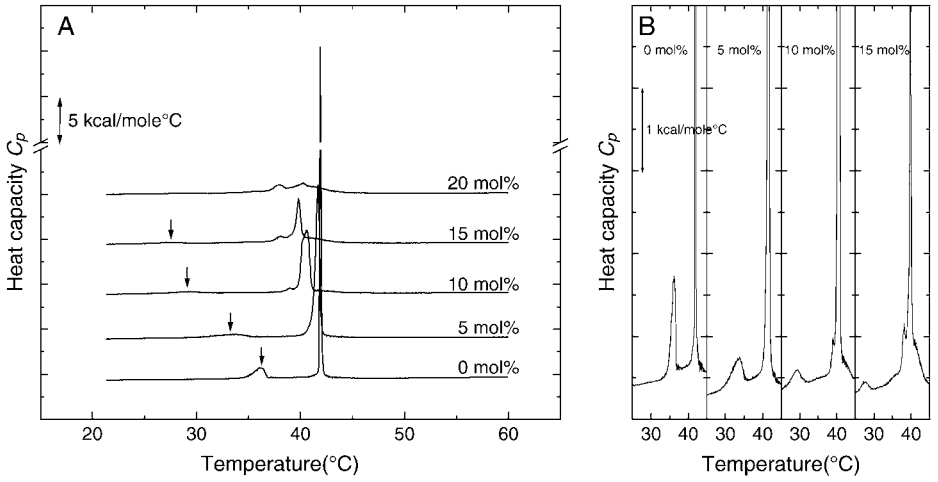

FIGURE 1 Heat capacity curves obtained by DSC at a scan rate of 30°C/h. (*A*) Multilamellar C_{14}-peptide/DPPC liposomes containing 0, 5, 10, 15, and 20 mol % of the C_{14}-peptide. Arrows indicate the position of the pretransition. (*B*) Magnifications of the heat capacity curves shown in *A* of multilamellar C_{14}-peptide/DPPC liposomes containing 0, 5, 10, and 15 mol % of the C_{14}-peptide.

TABLE 1 Variation of the main phase transition temperature, T_m, the transition enthalpy, ΔH, the half-height width of the transition, $T_{1/2}$, and the pretransition temperature, T_p, of the multilamellar liposomes composed of DPPC incorporated with increasing concentrations of the C_{14}-peptide

Mol % C_{14}-peptide	T_m (°C)	ΔH (kcal/mole)	$T_{1/2}$ (°C)	T_p (°C)
0	41.9	9.72	0.16	36.1
5	41.7	9.50	0.47	33.8
10	40.6	7.29	0.89	29.2
15	39.8	5.30	0.47	27.2
20	40.3	4.90	4.5	-

liposome preparation. Now we focus our attention on the effect of adding the C_{14}-peptide to the water phase of preformed liposomes. In Fig. 2, *A* and *B*, the C_{14}-peptide has been added to the water phase of preformed uni- and multilamellar DPPC liposomes just before starting the DSC scan. Unilamellar pure DPPC liposomes show a main phase transition at 41.3°C ($T_{1/2} = 1.4$°C, $\Delta H = 7.7$ kcal/mole). It is noted that $T_{1/2}$ for pure unilamellar DPPC liposomes (Fig. 2 *A*) is significantly larger than $T_{1/2}$ for the pure multilamellar liposomes (see Fig. 2 *B* and Table 1). The broadening of the heat capacity curves at the gel-to-fluid transition for the unilamellar DPPC liposomes as compared to the multilamellar liposomes reflects a change in the cooperative behavior of the many particle lipid membrane system (41). When 10% C_{14}-peptide is added to the water phase of preformed unilamellar DPPC liposomes, it is clearly seen that the main phase transition temperature is shifted to lower temperatures, $T_m = 40.4$°C, the enthalpy is diminished, $\Delta H = 6.9$ kcal/mole, and the transition takes place over a narrower temperature range, $T_{1/2} = 1.0$°C. In addition a second small peak that is only present in the consecutive upscan arises around 30°C. In unilamellar liposomes the pretransition is usually not observed, although in some cases it can be present (42). However, the peak appearing around 30°C corresponds to the pretransition of the DPPC multilamellar liposomes incorporated with 10 mol % of the C_{14}-peptide as shown in Fig. 1. We therefore suggest that this peak indicates a transition from the gel to the ripple phase of the unilamellar liposomes.

When the C_{14}-peptides are added to preformed multilamellar DPPC liposomes in concentrations of 10 mol %, two extra peaks appear in addition to the main phase transition peak at 41.9°C and the pretransition peak at 36.1°C. A new and sharp peak appears at 40.0°C just below the main phase transition temperature, and a very small peak appears around 29°C. It is furthermore of interest that the peak around 40°C for the multilamellar liposomes grows in size as the liposome suspension is taken through a series of up- and downscans as shown in Fig. 2 *C*. It has been shown experimentally by Papahadjopoulos et al. (43) and theoretically by Cruzeiro-Hansson and Mouritsen (44) that the transmembrane permeability displays a drastic increase at the main phase transition. Seen in this light a possible explanation of the multiple peaks in the DSC curves could be that the C_{14}-peptides migrate through the individual lamellae of the multilamellar DPPC liposomes layer by layer as the liposomes repeatedly are taken through the phase coexistence region. In the first DSC scan only the outermost layer of the multilamellar liposomes is in contact with the peptide. Since the peptide has a freezing point depression effect on the DPPC lipids, the lipid layer in contact with the peptide most likely melts at a slightly lower temperature than the unexposed lipid layers. Likewise, the appearance of a small peak around 30°C indicates that the lipids in the outermost layer are arranged in a ripple structure at the temperature range between 30°C and the main phase transition temperature. As the lipid-peptide mixture is taken through a series of up- and downscans, more and more DPPC lipids constituting the internal layers of the multilamellar system come into contact with the C_{14}-peptide. This results in an increased fraction of the DPPC molecules melting at 40°C and forming the ripple phase at 30°C.

Insertion of C_{14}-peptides into preexisting defect regions in supported gel phase DPPC bilayers

The lipid membrane structure was further characterized using AFM. In the topopgraphic AFM images, the topology

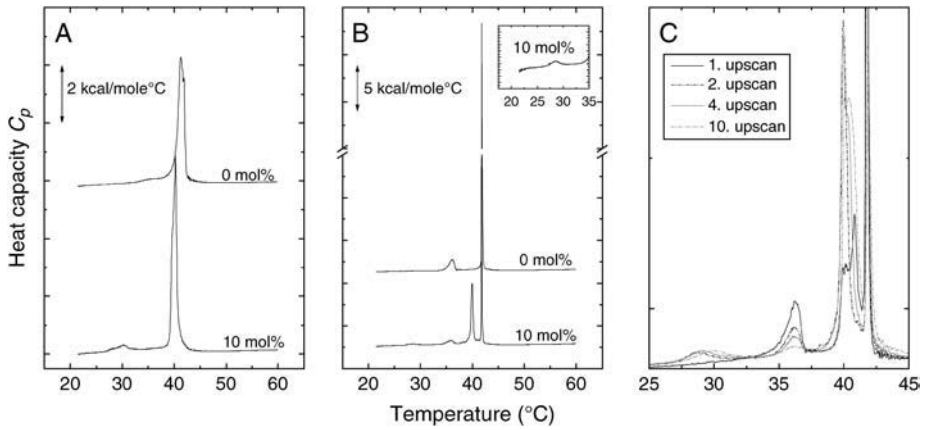

FIGURE 2 Heat capacity curves obtained by DSC at a scan rate of 30°C/h. (*A*) Unilamellar DPPC liposomes without (0 mol %) and with 10 mol % of the C_{14}-peptide added to the preformed liposomes from the water phase. (*B*) Multilamellar DPPC liposomes without and with 10 mol % of the C_{14}-peptide added from the water phase. The inset shows an enlargement of the low-enthalpy transition around 29°C. (*C*) Multilamellar DPPC liposomes with 10 mol % of the C_{14}-peptide added from the water phase. This liposome suspension was taken through a series of 10 up- and downscans. The first, second, fourth, and 10th upscans are shown.

of the lipid membrane is represented by a color scale (see inserted color scale on the images). On this scale, dark colors correspond to lower lying regions and light colors correspond to higher lying regions of the membrane. In general, the mica-supported DPPC lipid bilayer displays a smooth surface that often contains some defects as seen in Fig. 3 *A*. These defects can be used to determine the bilayer thickness, which in our experiments is ~6 nm (measured from the mica support to the top of the bilayer), in accordance with other studies (45,46). The narrow cracks can be clearly seen in the DPPC bilayer surface and are similar to cracks that have been reported in earlier studies (47). In Fig. 3 *B* we have added the C_{14}-peptide to the water phase of the preformed supported DPPC bilayer. Just after the addition of the peptides the crack zones are markedly affected, indicating that the C_{14}-peptide inserts predominantly into crack regions in the supported bilayer and thereby creates local membrane regions having a high peptide concentration. These peptide enriched regions follow the preexisting cracks and have ~10 Å smaller height than the surrounding lipids, indicating that the C_{14}-peptide has a membrane thinning effect.

Ripple appearance of DPPC lipids in the presence of C_{14}-peptides

To be able to observe the ripple phase in a supported bilayer membrane, one needs to have a freely floating bilayer on top of a bottom bilayer adsorbed to the smooth mica substrate (30,31,48–50). Therefore we used a newly established method for obtaining a second bilayer on top of a lower lying bilayer as described in the Materials and Methods section. It was observed that the presence of the C_{14}-peptide apparently facilitated the formation of double or multiple bilayers. Under identical sample conditions, pure DPPC lipids did not as readily form double or multiple bilayers.

Fig. 4 shows an image of a supported DPPC double lipid bilayer containing 10 mol % of the C_{14}-peptide. The ripple structure is seen in a lipid bilayer island on top of a lower lying supported bilayer of DPPC and C_{14}-peptide at 32°C (cooled from 37°C). The predominant periodicity of the ripples is ~30 nm, and the ripple structure has characteristic bending angles of 60° and 120° in accordance with other studies (51–54). Similarly, earlier studies have shown that

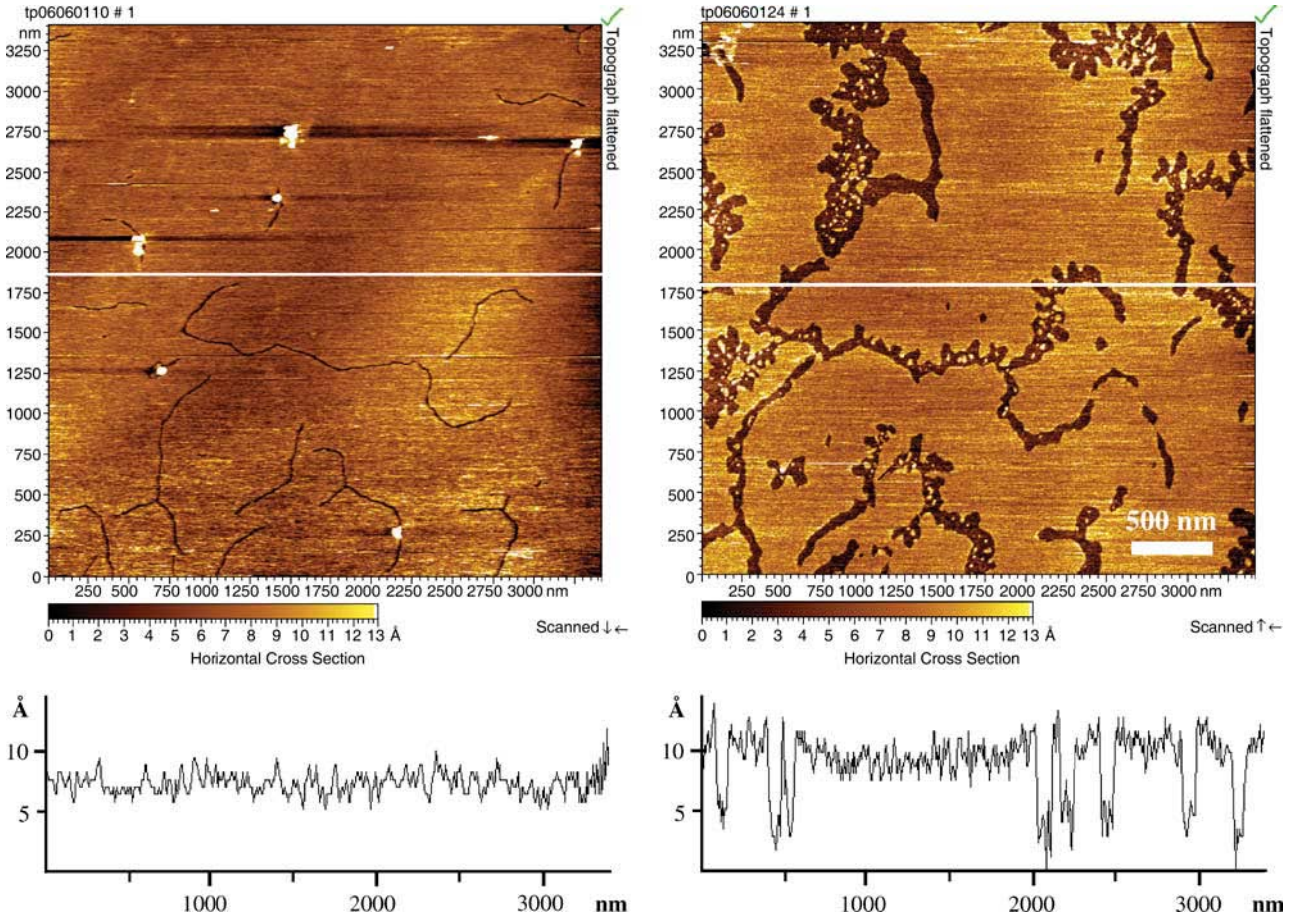

FIGURE 3 (*A*) AFM micrograph of a DPPC bilayer in the gel phase at 30°C on a solid support (mica). Defect lines are visible in the DPPC lipid bilayer. (*B*) The same DPPC bilayer as in *A* 100 min after C_{14}-peptide addition. It is seen that the C_{14}-peptide predominantly inserts into the defect zones, thereby creating local membrane regions with a high concentration of C_{14}-peptides. The height profile shows that these peptide-enriched membrane regions are ~10 Å lower than lipid bilayer regions that are unaffected by the peptide.

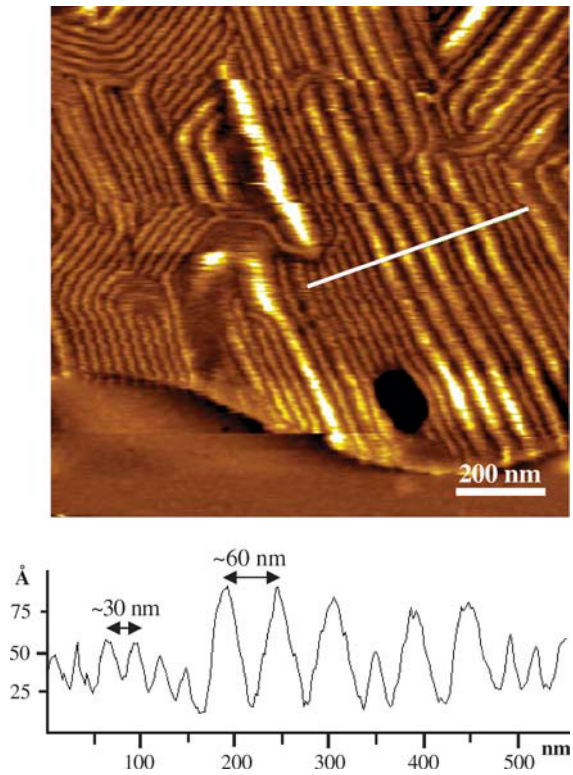

FIGURE 4 AFM image of supported double bilayers of DPPC lipids incorporated with 10 mol % of the C_{14}-peptide at 32°C. Ripples are seen in the upper bilayer. The height profile corresponds to the white line in the image and shows two characteristic ripple spacings of ~30 nm and ~60 nm. These ripple spacings are similar to pure DPPC lipid bilayers.

certain solutes and peptides like gramicidin A can induce ripple structures in supported layers (46,55). In addition to the 30 nm ripples, a few ripples having a periodicity of ~60 nm are also present. X-ray diffraction and electron microscopy on multilamellar PC bilayers show that the typical periodicity of bilayer ripples is either 12–16 nm or approximately double that value, depending on the thermal history (54,56,57). The short periodicity ripples form when entering the ripple phase temperature range by heating a lipid bilayer from the gel phase, and the long periodicity ripples form when cooling from the fluid phase. Similar to these observations for pure PC lipid bilayers, we observe the long periodicity of the ripple structure when the C_{14}-peptide/DPPC mixture was heated to 60°C then incubated at 37°C and imaged at 32°C. However, when the sample was kept at 4°C overnight, the ripples disappeared, and when the temperature was raised to 35°C, ripples with the short periodicity appeared (data not shown) in accordance with a previous report on pure DPPC lipid bilayers (31). The observation of the ~60 nm ripples may indicate that the C_{14}-peptide promotes the formation of this type of ripples. However, we have also occasionally seen this ripple periodicity in pure DPPC lipid bilayers, and the C_{14}-peptide did not result in a dramatic increase in the occurrence of the ~60 nm ripples.

By AFM, we also investigated how the ripple phase structure of DPPC membranes was affected by the addition of the C_{14}-peptide to the water phase of preformed supported DPPC bilayers. In Fig. 5 *A*, a lipid DPPC island on top of a supported DPPC bilayer is shown. Ripples with a periodicity of 30 nm appear in the upper bilayer island, and the structure of the underlying DPPC bilayer is planar. The AFM scan shown in Fig. 5 *B* was imaged 15 min after addition of the C_{14}-peptide to the water phase. The ripple periodicity of the upper bilayer island is 30 nm, and the ripple appearance is clearly unaffected by the presence of peptide. Fig. 5 *C* shows that when the island was repeatedly scanned the ripples apparently disappeared. However, when the scanning region was slightly moved, it was observed that ripples were still present in an island not previously scanned as shown in Fig. 5 *D*. This indicates that the force applied by the AFM tip is capable of erasing the ripples. This effect is not observed in pure DPPC lipid bilayers, which are stable toward AFM imaging. The effect is not related to peptide induced differences in ripple structure, as evidenced by the island that was not repeatedly scanned, and it was therefore concluded that the ripple appearance of DPPC membranes was unaffected by the C_{14}-peptide.

Appearance of coexisting lipid domains

Even though the ripple appearance was found to be unaffected by the presence of the C_{14}-peptide, the structure of the lower DPPC bilayer is dramatically affected. In Fig. 5 *A*, before the addition of peptides, the lower DPPC bilayer is planar. When the supported DPPC bilayers are imaged 15 min after peptide addition (Fig. 5 *B*), the structure of the underlying DPPC bilayer has changed into coexisting lipid domains characterized by a height difference of 10 Å corresponding to the height difference between gel and fluid phase DPPC lipids (58). By comparing Fig. 5 *B* with Fig. 5 *C* imaged 15 and 57 min after peptide addition, respectively, it can be seen that the shape of the domains is time dependent, starting with ramified structures that become more rounded with time. Interestingly, Rinia et al. (47) recently studied mixtures of DPPC lipids and the transmembrane Trp(W)-Ala(A)-Leu(L)-Pro(P) (WALP) peptide using AFM. These authors found that the transmembrane peptides in gel-state DPPC bilayers form line-type aggregates and that these aggregates cluster together in striated domains. Furthermore, the interaction of the surface-active lipopeptide surfactin-C_{15} with DPPC monolayers has also been investigated by AFM (59). The AFM topographic images revealed phase separation of the mixed DPPC-surfactin monolayers. The observed height difference between the surfactin and the DPPC domains of 12 Å was ascribed to differences in molecular orientation of the two different molecules, where the DPPC assumes a vertical position with the polar headgroup in contact with mica, with the large peptide ring of surfactin lying on the mica surface (60).

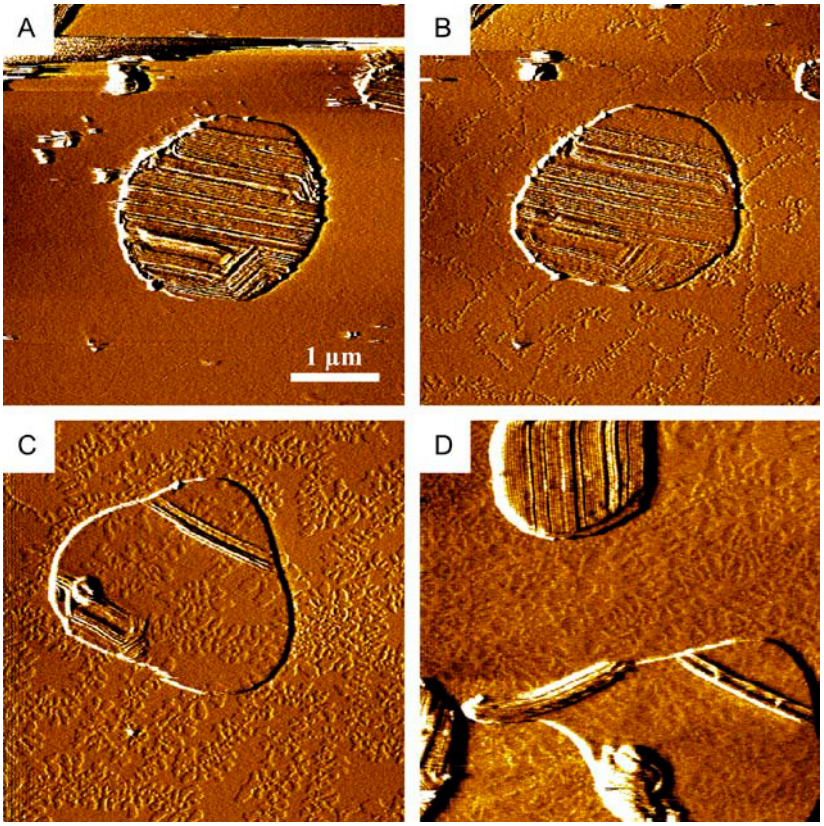

FIGURE 5 Addition of C_{14}-peptide to supported double bilayers of DPPC lipids in the ripple phase at 37°C. (*A*) Before addition of the C_{14}-peptide, ripples are present in the upper bilayer island. (*B*) 15 min after addition of the C_{14}-peptide. The ripples in the upper bilayer island are unaffected by the peptide addition, whereas the structure of the lower DPPC bilayer is clearly affected by the addition of the C_{14}-peptide. (*C*) 57 min after peptide addition, the ripples on the island have apparently disappeared. The underlying structure of the lower DPPC bilayer is markedly affected by the presence of the C_{14}-peptide. (*D*) Ripples still present in an island not previously scanned 110 min after C_{14}-peptide addition.

MD simulations

To obtain additional structural and dynamic information of the interaction of the C_{14}-peptide with DPPC lipid membranes, MD simulations were performed. In the MD simulations, the lipids and the peptide as well as the water are all represented in atomistic detail in terms of the CHARMM27 force field (36–38). We have recently published MD simulation results of the same system in greater detail (33). In this report, we focus the attention on particular aspects that can provide an explanation and support to the experimental observations. To estimate the change in bilayer lateral area and in lateral area compressibility due to the presence of the anchored peptide, we have previously demonstrated that it is in this regard feasible and convenient to subject the DPPC bilayers to an applied surface tension, γ, where 35 dyn/cm $\leq \gamma \leq$ 61 dyn/cm (33). This range of surface tensions ensures that our simulations capture gel- and fluid-like structures of the DPPC bilayer for the lowest and highest applied surface tensions, respectively. Moreover, this approach to some extent compensates for the lack of ability to study phase transitions using MD. A snapshot from our simulations with $\gamma = 61$ dyn/cm is displayed in Fig. 6 *A*. This snapshot shows the C_{14}-acyl chain anchored in the apolar part of the lipid bilayer while the tryptophan residue of the peptide is positioned in the headgroup region, and the rest of the peptide chain is in the water phase, in accord with the average behavior of these respective moieties. In particular, the location of the tryptophan residue in the headgroup region is highly stable (33). It has been argued that ripple phase formation takes place in large headgroup phospholipid when the relationship between the headgroup area and the cross sectional area of the acyl chains exceeds a certain threshold value (27,28). Keeping this in mind, the MD simulation data may provide an explanation to the extended temperature range of ripple phase formation, as the persistent location of the tryptophan residue in the lipid bilayer headgroup region is likely to lower the temperature where this threshold is exceeded.

From the applied surface tension simulations, we obtain within a 14 ns simulation time equilibrium areas of the DPPC bilayers in the presence (+) and absence (−) of the peptide. These areas, denoted $\bar{A}(DPPC^+)$ and $\bar{A}$ $(DPPC^-)$, respectively, with standard deviations $\sigma_{\bar{A}(DPPC+)} \equiv \sigma^+$ and $\sigma_{\bar{A}(DPPC-)} \equiv \sigma^-$ both increase linearly with γ (33). Now, we define the relative area $A'(\gamma) = \bar{A}(DPPC^+)/\bar{A}(DPPC^-) \equiv A^+(\gamma)/A^-(\gamma)$ with standard deviation $\sigma(\gamma_i) = [\sigma^+(\gamma_i)^2 (\partial_{A^+}A'(\gamma))^2|_{\gamma=\gamma_i} + \sigma^-(\gamma_i)^2(\partial_{A^-}A'(\gamma))^2|_{\gamma=\gamma_i}]^{1/2}$ where $\partial_{A^\pm} A'(\gamma) = \partial A'(\gamma)/\partial A^\pm$. Results including linear regression of $A'(\gamma)$ are shown in Fig. 6 *B*. We consistently find for all γ an area increase in $DPPC^+$ relative to $DPPC^-$ due to the presence of the peptide. Extrapolation to the limit of zero surface tension yields $\lim_{\gamma\to 0}A'(\gamma) = 1.28 \pm 0.11$, i.e.,

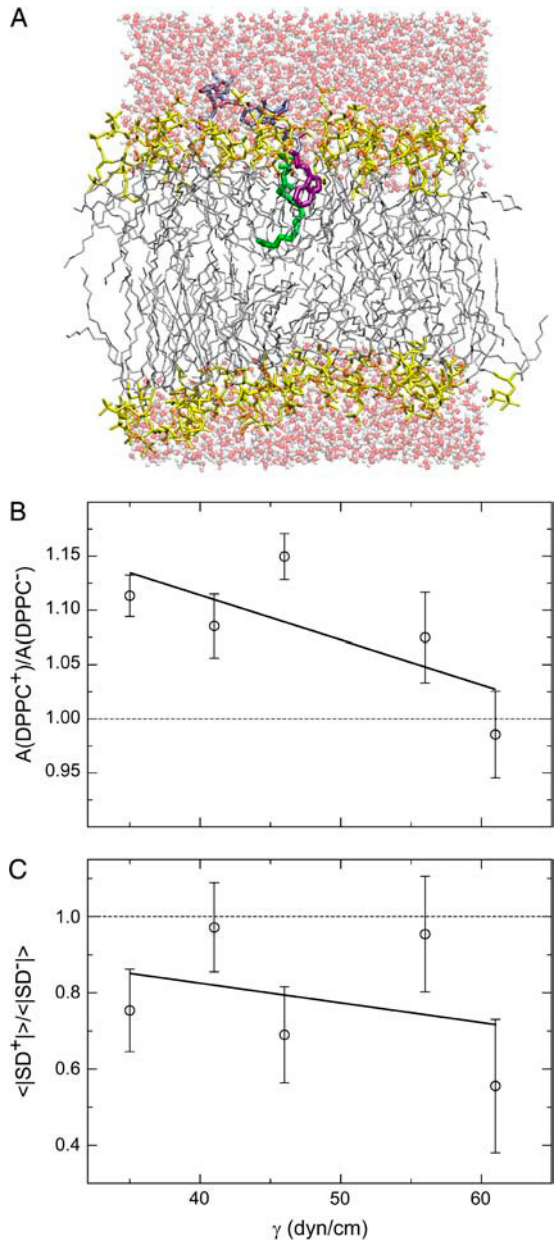

FIGURE 6 (*A*) Simulation snapshot of the peptide-DPPC system simulated with an applied surface tension of 61 dyn/cm. Modeling and simulation details are provided in Jensen et al. (33). The choline headgroup and the palmitoyl chains are colored yellow and gray, respectively. Water molecules appear in red and white. The peptide-C_{14} anchor is colored green. The interfacial tryptophan residue is displayed in purple, and the remainder of the peptide appear in ice blue. (*B*) Equilibrium areas $A'(\gamma) = \bar{A}(DPPC^+)/\bar{A}(DPPC^-) \equiv A^+(\gamma)/A^-(\gamma)$ of the DPPC bilayer with the anchored peptide (+) relative to pure DPPC lipid bilayers (−) as a function of applied surface tension. Average areas were for all γ computed in the time interval 10–14 ns. Errors in the equilibrium area were obtained as $\sigma(\gamma_i) = [\sigma^+(\gamma_i)^2(\partial_{A^+}A'(\gamma))^2|_{\gamma=\gamma_i} + \sigma^-(\gamma_i)^2(\partial_{A^-}A'(\gamma))^2|_{\gamma=\gamma_i}]^{1/2}$ where $\partial_{A^\pm}A'(\gamma) = \partial A'(\gamma)/\partial A^\pm$. (*C*) Average relative deuterium order parameter $\langle|SD|'(\gamma)\rangle = \langle|SD|(\gamma)\rangle^+/\langle|SD|(\gamma)\rangle^-$ of peptide-containing (+) and peptide-free (−) DPPC bilayers displayed as a function of applied surface tension. Averages and errors were computed as in (*A*). The phase-structure of the bilayer approaches gel- and fluid-like characteristics with decreasing and increasing γ, respectively, in panels *B* and *C*.

roughly a 30% peptide-induced increase in lateral area, and $\lim_{\gamma\to 70\text{dyn/cm}} A'(\gamma) \cong 1$ since excess area available for peptide incorporation gradually vanishes as tensions of increasing magnitude are applied (overstretching occurs for a limiting tension $\gamma \cong 70$ dyn/cm (33)). Clearly, the 30% area expansion owing to incorporation of the peptide is associated with quite large statistical uncertainty (~40%). Given that relative large surface tensions are needed to maintain the bilayers in stable fluid states in our simulations, resorting to the current choice of simulation parameters and macroscopic boundary conditions (33), we therefore expect that the 30% expansion is an upper limit of this lateral dilution effect. Nevertheless, the (large) lateral area expansion suggested by the MD simulations results in a decrease in the membrane thickness as the lipid bilayer volume is expected to be fairly constant, and the simulations therefore qualitatively agree with the membrane thinning effect of the C_{14}-peptide observed in our AFM experiments. In addition to area expansion, peptide anchoring also affects structural order of the bilayer hydrocarbon core relative to pure DPPC bilayers according to lipid deuterium order parameter profiles $|SD|'$ resolved along the fatty acid chains for $DPPC^\pm$ (33). Even across the bilayer core, i.e., also in the monolayer devoid of peptide in $DPPC^+$, acyl disorder increases (33), which also is supportive of the large area increase in $DPPC^+$ relative to $DPPC^-$ as observed above. For this discussion, we report as a function of γ an average deuterium order parameter $\langle|SD|'(\gamma)\rangle^\pm$ where $\langle \ldots \rangle$ indicate the average over all methylenic groups in the palmitoyl chains and $\pm$ has the same meaning as above. As to be expected, we consistently find for $DPPC^\pm$ a linear decrease of $\langle|SD|'(\gamma)\rangle^\pm$ with γ accompanying the increase in the bilayer lateral area above. The peptide-induced changes in bilayer structural order relative to the pure bilayer $\langle|SD|'(\gamma)\rangle = \langle|SD|(\gamma)\rangle^+/\langle|SD|(\gamma)\rangle^-$ with standard deviation $\sigma_{|SD|(\gamma)}$ may be obtained analogously to the relative area $A'(\gamma)$ above, given a linear decrease of $\langle|SD|(\gamma)\rangle^\pm$ with γ. Results for the relative average order parameter $\langle|SD|'(\gamma)\rangle$, including linear regression, are shown in Fig. 6 *C*. As seen, $\langle|SD|'(\gamma)\rangle$ is consistently below unity for any γ, indicating that for any phase structure of the bilayer, the peptide induces disorder in the bilayer hydrocarbon core while the magnitude of the induced disorder decreases with increasing γ. The increased disorder caused by the C_{14}-peptide will have a fluidizing effect on the lipid bilayer and is therefore consistent with the lowering of the main phase transition temperature that was observed in our DSC measurements.

CONCLUSION

The DSC results in this study have demonstrated that the C_{14}-peptide has a pronounced influence on the phase behavior of multilamellar DPPC liposomes. This was manifested as a decrease in the transition enthalpy and a downshift in the transition temperature of the main phase transition and the

pretransition, as well as a concomitant broadening of both transitions. The AFM experiments showed that when the C_{14}-peptide was added to supported gel phase DPPC bilayers from the water phase, it inserted predominantly into preexisting defect regions in the bilayer and displayed a membrane thinning effect on the surrounding lipids. In addition, it was found that the ripple structure in double supported bilayers is preserved in C_{14}-peptide/DPPC mixtures with the characteristic ripple periodicity as observed in pure DPPC membranes. Although the ripple appearance of DPPC bilayers was unaffected by the presence of the C_{14}-peptide, the AFM experiments are, due to the corrugation, not accurate enough to assess possible changes in the bilayer thickness and details in the lateral structure. However, the effect of C_{14}-peptide on the lipid bilayer can readily be seen in the structure of the first planar DPPC bilayer, which due to the support is smoother. We find that this layer was highly affected by the C_{14}-peptide, resulting in coexisting lipid domains characterized by a 10 Å height difference. MD simulations showed a disordering effect of the C_{14}-peptide accompanied by a lateral area expansion, which supported both the membrane thinning effect seen in the AFM experiments as well as the lowering of the main phase transition temperature observed by DSC. Furthermore, the simulations demonstrated a tendency of the tryptophan residue of the peptide to position itself in the headgroup region of the lipid bilayer (33). This location of tryptophan could possibly explain the expanded temperature range of ripple phase formation.

Computing time at the Danish Center for Scientific Computing is gratefully acknowledged.

This work was supported by the Apoteker Foundation of 1991, by the Hasselblad Foundation, and by the Danish Medical Research Council via a grant to the Center for Drug Design and Transport. MEMPHYS—Center for Biomembrane Physics is supported by the Danish National Research Foundation.

REFERENCES

1. Resh, M. D. 1999. Fatty acylation of proteins: new insights into membrane targeting of myristoylated and palmitoylated proteins. *Biochim. Biophys. Acta.* 1451:1–16.
2. Silvius, J. R. 1999. Lipid modifications of intracellular signal-transducing proteins. *J. Liposome Res.* 9:1–19.
3. Mouritsen, O. G. (2005). Life—As a Matter of Fat. The Emerging Science of Lipidomics. Springer-Verlag, Heidelberg, Germany.
4. McLaughlin, A., and A. Aderem. 1995. The myristoyl-electrostatic switch: a modulator of reversible protein-membrane interactions. *Trends Biochem. Sci.* 20:272–276.
5. Dell'aqua, M. L., and J. D. Scott. 1997. Protein kinase A anchoring. *J. Biol. Chem.* 272:12881–12884.
6. Murray, D., A. Arbuzova, B. Honig, and S. McLaughlin. 2002. The role of electrostatic and nonpolar interactions in the association of peripheral proteins with membranes. *Curr. Top. Membr.* 52:271–302.
7. Liang, X., A. Nazarian, H. Erdjument-Bromage, W. Bornmann, P. Tempst, and M. D. Resh. 2004. Heterogeneous fatty acylation of Src family kinases with polyunsaturated fatty acids regulates raft localization and signal transduction. *Proc. Natl. Acad. Sci. USA.* 101: 1880–1885.
8. Wang, J., D. Shen, and W. C. Shen. 1999. Preparation, purification, and characterization of a reversibly lipidized desmopressin with potentiated anti-diuretic activity. *Pharm. Res.* 16:1674–1679.
9. Kurtzhals, P., S. Havelund, I. Jonassen, B. Kiehr, U. D. Larsen, U. Ribel, and J. Markussen. 1995. Albumin binding of insulins acylated with fatty acids: characterization of the ligand protein interaction and correlation between binding affinity and timing of the insulin effect in vivo. *Biochem. J.* 312:725–731.
10. Simons, K., and E. Ikonen. 1997. Functional rafts in cell membranes. *Nature.* 387:569–572.
11. Jacobson, K., and C. Dietrich. 1999. Looking at lipid rafts? *Trends Cell Biol.* 9:87–91.
12. Pralle, A., P. Keller, E. L. Florin, K. Simons, and J. K. H. Horber. 2000. Sphingolipid-cholesterol rafts diffuse as small entities in the plasma membrane of mammalian cells. *J. Cell Biol.* 148:997–1007.
13. Brown, D. A. 2001. Seeing is believing: visualization of rafts in model membranes. *Proc. Natl. Acad. Sci. USA.* 98:10517–10518.
14. Burack, W. R., and R. L. Biltonen. 1994. Lipid bilayer heterogeneities and modulation of phospholipase A2 activity. *Chem. Phys. Lipids.* 73:209–222.
15. Yang, L., and M. Glaser. 1995. Membrane domains containing phosphatidylserine and substrate can be important for the activation of protein-kinase-C. *Biochemistry.* 34:1500–1506.
16. Lee, A. G. 2003. Lipid-protein interactions in biological membranes: a structural perspective. *Biochim. Biophys. Acta.* 1612:1–40.
17. Dowhan, W., E. Mileykovskaya, and M. Bogdanov. 2004. Diversity and versatility of lipid-protein interactions revealed by molecular genetic approaches. *Biochim. Biophys. Acta.* 1666:19–39.
18. Hønger, T., K. Jørgensen, R. L. Biltonen, and O. G. Mouritsen. 1996. Systematic relationship between phospholipase A(2) activity and dynamic lipid bilayer microheterogeneity. *Biochemistry.* 35:9003–9006.
19. Hønger, T., K. Jørgensen, D. Stokes, R. L. Biltonen, and O. G. Mouritsen. 1997. Phospholipase A(2) activity and physical properties of lipid-bilayer substrates. *Methods Enzymol.* 286:168–190.
20. Jørgensen, K., J. H. Ipsen, O. G. Mouritsen, and M. J. Zuckermann. 1993. The effect of anesthetics on the dynamic heterogeneity of lipid-membranes. *Chem. Phys. Lipids.* 65:205–216.
21. Barry, J. A., and K. Gawrisch. 1995. Effects of ethanol on lipid bilayers containing cholesterol, gangliosides, and sphingomyelin. *Biochemistry.* 34:8852–8860.
22. Mortensen, K., W. Pfeiffer, E. Sackmann, and W. Knoll. 1988. Structural properties of a phosphatidylcholine-cholesterol system as studied by small-angle neutron scattering: ripple structure and phase diagram. *Biochim. Biophys. Acta.* 945:221–245.
23. Tomoaia-Cotisel, M., and I. W. Levin. 1997. Thermodynamic study of the effects of ursodeoxycholic acid and ursodeoxycholate on aqueous dipalmitoyl phosphatidylcholine bilayer dispersions. *J. Phys. Chem. B.* 101:8477–8485.
24. Mavromoustakos, T., E. Theodoropoulou, and D. P. Yang. 1997. The use of high-resolution solid-state NMR spectroscopy and differential scanning calorimetry to study interactions of anaesthetic steroids with membrane. *Biochim. Biophys. Acta.* 1328:65–73.
25. Prenner, E. J., R. N. A. H. Lewis, L. H. Kondejewski, R. S. Hodges, and R. N. McElhaney. 1999. Differential scanning calorimetric study of the effect of the antimicrobial peptide gramicidin S on the thermotropic phase behavior of phosphatidylcholine, phosphatidylethanolamine and phosphatidylglycerol lipid bilayer membranes. *Biochim. Biophys. Acta.* 1417:211–223.
26. Tardieu, A., V. Luzzati, and F. C. Reman. 1973. Structure and polymorphism of the hydrocarbon chains of lipids: a study of lecithin-water phases. *J. Mol. Biol.* 75:711–733.
27. Carlson, J. M., and J. P. Sethna. 1987. Theory of the ripple phase in hydrated phospholipid bilayers. *Phys. Rev. A.* 36:3359–3374.
28. Kirchner, S., and G. Cevc. 1994. On the origin of thermal L(beta′)-P(beta′) pretransition in the lamellar phospholipid-membranes. *Europhys. Lett.* 28:31–36.

29. Pedersen, T. B., M. C. Sabra, S. Frokjaer, O. G. Mouritsen, and K. Jørgensen. 2001. Association of acylated cationic decapeptides with dipalmitoylphosphatidylserine-dipalmitoylphosphatidylcholine lipid membranes. *Chem. Phys. Lipids.* 113:83–95.

30. Leidy, C., T. Kaasgaard, J. H. Crowe, O. G. Mouritsen, and K. Jørgensen. 2002. Ripples and the formation of anisotropic lipid domains: imaging two-component supported double bilayers by atomic force microscopy. *Biophys. J.* 83:2625–2633.

31. Kaasgaard, T., C. Leidy, J. H. Crowe, O. G. Mouritsen, and K. Jørgensen. 2003. Temperature-controlled structure and kinetics of ripple phases in one- and two-component supported lipid bilayers. *Biophys. J.* 85:350–360.

32. Leidy, C., O. G. Mouritsen, K. Jørgensen, and G. H. Peters. 2004. Evolution of a rippled membrane during phospholipase A(2) hydrolysis studied by time-resolved AFM. *Biophys. J.* 87:408–418.

33. Jensen, M. Ø., O. G. Mouritsen, and G. H. Peters. 2004. Simulations of a membrane-anchored peptide: structure, dynamics, and influence on bilayer properties. *Biophys. J.* 86:3556–3575.

34. Hope, M. J., M. B. Bally, G. Webb, and P. R. Cullis. 1985. Production of large unilamellar vesicles by a rapid extrusion procedure. Characterization of size distribution, trapped volume and ability to maintain a membrane potential. *Biochim. Biophys. Acta.* 812:55–65.

35. Kale, L., R. Skeel, M. Bhandarkar, R. Brunner, A. Gursoy, N. Krawetz, J. Phillips, A. Shinozaki, K. Varadarajan, and K. Schulten. 1999. NAMD2: greater scalability for parallel molecular dynamics. *J. Comput. Phys.* 151:283–312.

36. Schlenkrich, M., J. Brickmann, A. D. MacKerrell Jr., and M. Karplus. 1996. An empirical potential energy function for phospholipids: criteria for parameter optimization and applications. *In* Biological Membranes: A Molecular Perspective from Computation and Experiment. K. M. Merz Jr. and B. Roux, editors. Birkhäuser, Boston. 31–81.

37. MacKerell, A. D., D. Bashford, M. Bellott, R. L. Dunbrack, J. D. Evanseck, M. J. Field, S. Fischer, J. Gao, H. Guo, S. Ha, D. Joseph-McCarthy, L. Kuchnir, K. Kuczera, F. T. K. Lau, C. Mattos, S. Michnick, T. Ngo, D. T. Nguyen, B. Prodhom, W. E. Reiher, B. Roux, M. Schlenkrich, J. C. Smith, R. Stote, J. Straub, M. Watanabe, J. Wiorkiewicz-Kuczera, D. Yin, and M. Karplus. 1998. All-atom empirical potential for molecular modeling and dynamics studies of proteins. *J. Phys. Chem. B.* 102:3586–3616.

38. Feller, S. E., and A. D. MacKerell. 2000. An improved empirical potential energy function for molecular simulations of phospholipids. *J. Phys. Chem. B.* 104:7510–7515.

39. Feller, S. E., and R. W. Pastor. 1999. Constant surface tension simulations of lipid bilayers: the sensitivity of surface areas and compressibilities. *J. Chem. Phys.* 111:1281–1287.

40. Wang, X. Y., K. Semmler, W. Richter, and P. J. Quinn. 2000. Ripple phases induced by alpha-tocopherol in saturated diacylphosphatidylcholines. *Arch. Biochem. Biophys.* 377:304–314.

41. Freire, E., and R. L. Biltonen. 1978. Estimation of molecular averages and equilibrium fluctuations in lipid bilayer systems from excess heat capacity function. *Biochim. Biophys. Acta.* 514:54–68.

42. Lichtenberg, D., M. Menashe, S. Donaldson, and R. L. Biltonen. 1984. Thermodynamic characterization of the pretransition of unilamellar dipalmitoylphosphatidylcholine vesicles. *Lipids.* 19:395–400.

43. Papahadjopoulos, D., K. Jacobson, S. Nir, and T. Isac. 1973. Phase transitions in phospholipid vesicles. Fluorescence polarization and permeability measurements concerning effect of temperature and cholesterol. *Biochim. Biophys. Acta.* 311:330–348.

44. Cruzeiro-Hansson, L., and O. G. Mouritsen. 1988. Passive ion permeability of lipid-membranes modelled via lipid-domain interfacial area. *Biochim. Biophys. Acta.* 944:63–72.

45. Tamm, L. K., and H. M. McConnell. 1985. Supported phospholipid bilayers. *Biophys. J.* 47:105–113.

46. Mou, J. X., J. Yang, and Z. F. Shao. 1994. Tris(hydroxymethyl)aminomethane (C4H11NO3) induced a ripple phase in supported unilamellar phospholipid-bilayers. *Biochemistry.* 33:4439–4443.

47. Rinia, H. A., R. A. Kik, R. A. Demel, M. M. Snel, J. A. Killian, J. P. van der Eerden, and B. de Kruijff. 2000. Visualization of highly ordered striated domains induced by transmembrane peptides in supported phosphatidylcholine bilayers. *Biochemistry.* 39:5852–5858.

48. Fang, Y., and J. Yang. 1996. Role of the bilayer-bilayer interaction on the ripple structure of supported bilayers in solution. *J. Phys. Chem.* 100:15614–15619.

49. Fragneto, G., T. Charitat, F. Graner, K. Mecke, L. Perino-Gallice, and E. Bellet-Amalric. 2001. A fluid floating bilayer. *Europhys. Lett.* 53: 100–106.

50. Kaasgaard, T., C. Leidy, J. H. Ipsen, O. G. Mouritsen, and K. Jørgensen. 2001. In situ atomic force microscope imaging of supported lipid bilayers. *Single Mol.* 2:105–108.

51. Ververgaert, P. H. J., A. J. Verkleij, P. F. Elbers, and L. L. M. van Deenen. 1973. Analysis of the crystallization process in lecithin liposomes: a freeze-etch study. *Biochim. Biophys. Acta.* 311:320–329.

52. Hicks, A., M. Dinda, and M. A. Singer. 1987. The ripple phase of phosphatidylcholines—Effect of chain-length and cholesterol. *Biochim. Biophys. Acta.* 903:177–185.

53. Meyer, H. W. 1996. Pretransition-ripples in bilayers of dipalmitoylphosphatidylcholine: undulation or periodic segments? A freeze-fracture study. *Biochim. Biophys. Acta.* 1302:138–144.

54. Katsaras, J., S. Tristram-Nagle, Y. Liu, R. L. Headrick, E. Fontes, P. C. Mason, and J. F. Nagle. 2000. Clarification of the ripple phase of lecithin bilayers using fully hydrated, aligned samples. *Phys. Rev. E.* 61:5668–5677.

55. Mou, J., D. M. Czajkowsky, and Z. Shao. 1996. Gramicidin A aggregation in supported gel state phosphatidylcholine bilayers. *Biochemistry.* 35:3222–3226.

56. Tenchov, B. G., H. Yao, and I. Hatta. 1989. Time-resolved x-ray-diffraction and calorimetric studies at low scan rates. 1. Fully hydrated dipalmitoylphosphatidylcholine (DPPC) and DPPC/water ethanol phases. *Biophys. J.* 56:757–768.

57. Koynova, R., A. Koumanov, and B. Tenchov. 1996. Metastable rippled gel phase in saturated phosphatidylcholines: calorimetric and densitometric characterization. *Biochim. Biophys. Acta.* 1285:101–108.

58. Cevc, G., and D. Marsh. 1987. Phospholipid Bilayers. Physical Principles and Models. John Wiley & Sons, New York.

59. Deleu, M., M. Paquot, P. Jacques, P. Thonart, Y. Adriaensen, and Y. F. Dufrene. 1999. Nanometer scale organization of mixed surfactin/phosphatidylcholine monolayers. *Biophys. J.* 77:2304–2310.

60. Sperotto, M. M., and O. G. Mouritsen. 1991. Monte-Carlo simulation studies of lipid order parameter profiles near integral membrane proteins. *Biophys. J.* 59:261–270.